System size dependence in backward relativistic hadron production in pA and AA collisions

B. M. Badawy[1)]

Reactor Physics Department, Nuclear Research Center, Atomic Energy Authority, Cairo, Egypt

Abstract: In this comprehensive study the multiplicity characteristics of the backward emitted relativistic hadron (shower particle) through hadron-nucleus and nucleus-nucleus are overviewed in three dimensions. These dimensions are the projectile size, target size, and energy. To confirm the universality in this production system, wide ranges of system size and energy ($E_{\rm lab}\sim$2.1 A up to 200 A GeV) are used. The multiplicity characteristics of this hadron imply a limiting behavior with respect to the projectile size and energy. The target size is the main effective parameter in this production system. The exponential decay shapes is a characteristic feature of the backward shower particle multiplicity distributions. The decay constant changes with the target size to be nearly 2.02, 1.41, and 1.12 for the interactions with CNO, Em, and AgBr nuclei, respectively, irrespective of the projectile size and energy. While the backward production probability and average multiplicity are constants at different projectile sizes and energies, they can be correlated with the target size in power law relations.

Key words: backward relativistic hadron, dubna energy and SPS energy, multiplicity characteristics, system size, nuclear limiting fragmentation

PACS: 25.75.-q, 25.75.Dw, 25.75.Gz **DOI:** 10.1088/1674-1137/38/11/114001

1 Introduction

From a kinematical point of view, the hadron emission in the backward hemisphere, (BHS), that is at $\theta_{\rm lab} \geqslant 90^\circ$, is restricted in the center of mass system. Accordingly, the pion production was investigated according to the directional zone of emission. Various experimental and theoretical studies had been focused at Dubna and Lawrence Berkeley National Laboratory (LBNL) to solve the problem [1–4]. El-Nadi et al [5–7] showed that the backward emitted pion multiplicity is strongly correlated with the target fragment multiplicity at Dubna energy. The pion production was investigated in relativistic and ultrarelativistic collisions, underlying their zonal emission influence at, $\theta_{\rm lab}<90^\circ$, forward hemisphere (FHS) [8–12]. These results suggested that the forward emitted pions originate from a source of particle creation system as a result of a fireball nuclear matter or hadronic matter decay. Otherwise, the backward emitted pions result from an exact decay system of the excited target nucleus in a later stage after the production of the forward ones. At Dubna energy, Abdelsalm et al [10] predicted the emission system temperature in the FHS and BHS is 112 and 27 MeV, respectively. It was suggested by Baldin et al [1] that the backward emission system of pion works at the onset of the target limiting fragmentation mechanism. Therefore, the predicted temperature of this backward emission system is expected to be constant at any energy or system size while the forward one must be changed with both of them. In experiment [12], the results suggest that there are two production mechanisms: fragmentation and pionization. The forward emitted hadrons originate from an emission system that is working in the pionization region, while the backward ones are formed in the target fragmentation region, regarding the nuclear limiting fragmentation hypothesis beyond 1 A GeV [13].

According to the commonly used nuclear emulsion terminology [14, 15], the shower tracks emitted in the 4-π space are identified as relativistic hadrons where the lower boundary of their kinetic energy spectrum is usually taken to be 400 MeV. The majority of these hadrons (more than 90%) are pions [10, 16–20]. They are separated from the non-interacting singly charged projectile fragments (protons, deuterons, and tritons) and are differentiated from them. Therefore, pions are regarded as the major fraction part of the produced relativistic hadrons in photographic nuclear emulsion experiments.

In the present experiment, the emission characteristics of the relativistic hadron in the BHS are studied at a wide range of system sizes. The case of hadron-nucleus interaction has been given in p interaction with emulsion

Received 4 December 2013

1) E-mail: he_cairo@yahoo.com

nuclei. The light projectile nuclei are presented by ^{3}He, ^{4}He, ^{6}Li, and ^{7}Li. The interactions of ^{24}Mg, ^{28}Si, and ^{32}S with emulsion nuclei are examples of heavy-ion collisions. The emulsion nuclei can cover targets with mass numbers of $A_{\rm T}$=1 up to 108. The dependence on the incident energy is also considered where the used range of $E_{\rm lab}$ is 2.1 A up to 200 A GeV. This energy domain extends widely beyond the onset of the nuclear limiting fragmentation region. The used data are from the data bank of the Mohamed El-Nadi high energy lab, Faculty of Science, Cairo University, Egypt.

2 Experimental details

2.1 Technique

The methods, equipments, and experimental restrictions used are similar to those detailed in Ref. [12]. The nuclear emulsions compositions, the statistical information, and the measured mean free paths can be found in Ref. [21].

The produced particles are identified in photographic nuclear emulsion according to the commonly accepted ionization behavior [14, 15] as:

(1) Shower particles having $g\leqslant 1.5g_{\rm p}$, where g is the track grain density and $g_{\rm p}$ corresponds to the grain density of the minimum ionizing track. These particles are relativistic hadrons, which consist mainly of pions and less than 10% are other mesons and baryons. Their multiplicity is denoted as $n_{\rm s}$. The notations $n_{\rm s}^{\rm f}$ and $n_{\rm s}^{\rm b}$ correspond to the shower particles emitted in the FHS and BHS, respectively. The backward emitted ones are interested herein.

(2) Grey particles having a range >3 mm and $1.5g_{\rm p}< g\leqslant 4.5g_{\rm p}$, which are mainly recoil protons knocked-out from the target nucleus during the collision. Their kinetic energy ranges from 26 up to 400 MeV.

(3) Black particles having a range $\leqslant$3 mm and $g> 4.5g_{\rm p}$, which are evaporated target protons with kinetic energy <26 MeV.

(4) The grey and black particles together amount to the group of the target fragments, the so called heavily ionizing particles. These fragments are emitted in the 4-π space. Their multiplicity is denoted as $N_{\rm h}$

(5) Projectile fragments having $Z\geqslant 1$, which are fragmented nuclei having nearly the same momentum of the incident nucleus. They are emitted in a very narrow forward cone along the direction of incidence.

2.2 Target nuclei discrimination

The nuclear emulsion is composed of a homogeneous mixture of nuclei. The chemical composition of nuclear emulsion is H, C, N, O, Br, and Ag. Their densities correspond to those given in Ref. [21]. The target size is usually determined in terms of the mass number, $A_{\rm T}$. The effective target is recognized, event by event, statistically. Accordingly, the total sample of events is discriminated into groups in which adequate statistics are enclosed. They correspond to H nuclei, CNO (the light target), Em (the nuclear emulsion as a whole), and AgBr (the heavy target). The effective masses of these groups of target nuclei are determined as 1, 14, 70, and 94, respectively [22]. The different experimental and theoretical methods for target nuclei discriminations are detailed in Ref. [12, 21, 23–26]. In the present experiment, the fraction of each target is simulated theoretically using the Glauber's approach encoded in Ref. [27].

3 Experimental results

3.1 Multiplicity Distributions

Figure 1 through Fig. 3 present the multiplicity distributions of the backward emitted shower particles in the interactions of p, ^{3}He, ^{4}He, ^{6}Li, ^{7}Li, ^{24}Mg, ^{28}Si, and ^{32}S with CNO, Em, and AgBr nuclei at energy range (2.1 A up to 200 A GeV). The characteristic feature of the distributions is the exponential decay shape, irrespective of the energy or system size. The data are well approximated by the exponential decay law of Eq. (1) and

Table 1. The fit parameters characterizing the backward emitted shower particle multiplicity distributions in the present interactions with emulsion nuclei.

target		CNO		Em		AgBr	
projectile	$E_{\rm lab}/A$ GeV	p_0	λ	p_0	λ	p_0	λ
p	3.7	85.59±3.38	1.98±0.08	80.95±1.70	1.73±0.04	78.68±1.99	1.65±0.04
^{3}He	3.7	87.73±4.05	2.10±0.11	78.09±2.08	1.54±0.04	73.14±2.47	1.21±0.04
^{4}He	2.1	88.53±3.73	2.17±0.11	81.65±1.95	1.71±0.04	77.55±0.02	1.52±0.05
	3.7	84.00±4.96	1.84±0.12	74.04±2.52	1.35±0.05	68.44±2.98	1.16±0.05
^{6}Li	3.7	85.17±4.98	1.91±0.12	71.15±2.53	1.25±0.04	63.96±2.96	1.05±0.04
^{7}Li	2.2	86.75±5.08	2.02±0.14	77.22±2.74	1.48±0.06	70.76±3.31	1.22±0.06
^{24}Mg	3.7	85.54±4.58	1.95±0.12	73.06±2.53	1.34±0.05	62.08±3.09	0.99±0.04
^{28}Si	3.7	85.53±4.53	1.92±0.12	71.95±2.40	1.28±0.04	60.59±2.90	0.99±0.04
	14.6	82.67±6.48	1.79±0.16	67.76±3.45	1.19±0.06	55.95±4.08	0.83±0.06
^{32}S	3.7	89.52±6.52	2.25±0.20	68.04±3.14	1.15±0.05	54.24±3.51	0.77±0.05
	200	89.19±4.30	2.24±0.13	74.05±2.31	1.47±0.05	59.20±2.73	0.93±0.05

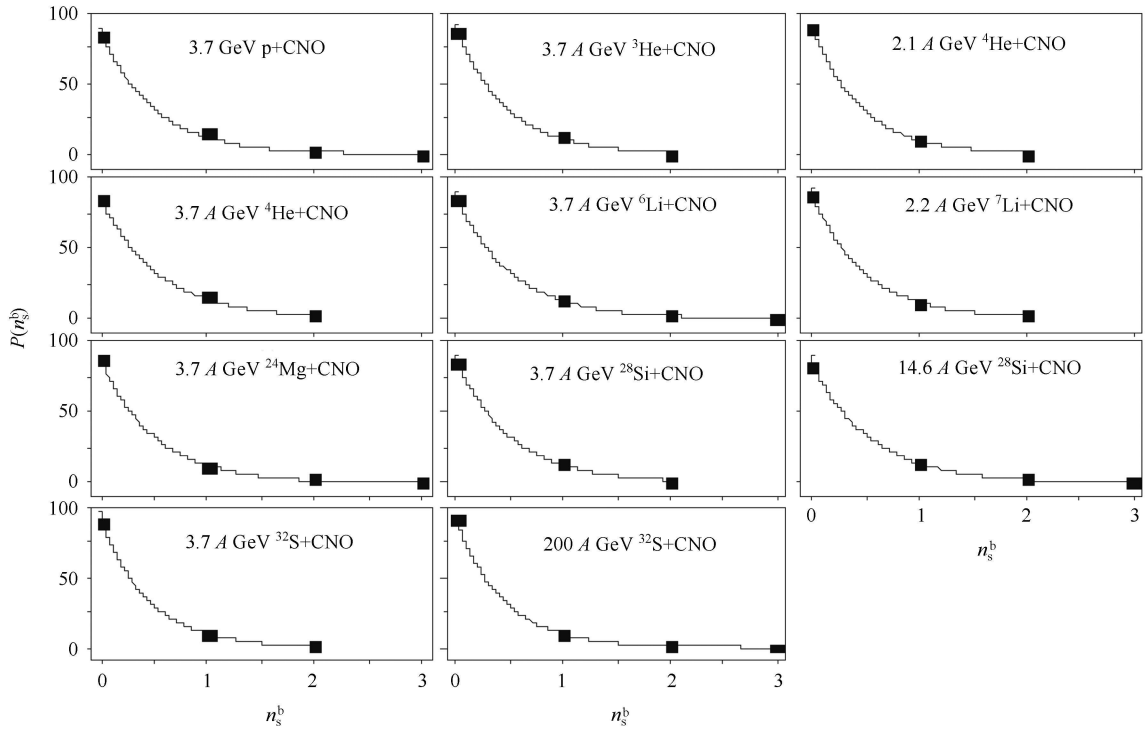

Fig. 1. The multiplicity distributions of the backward emitted shower particle together with the fitted curves.

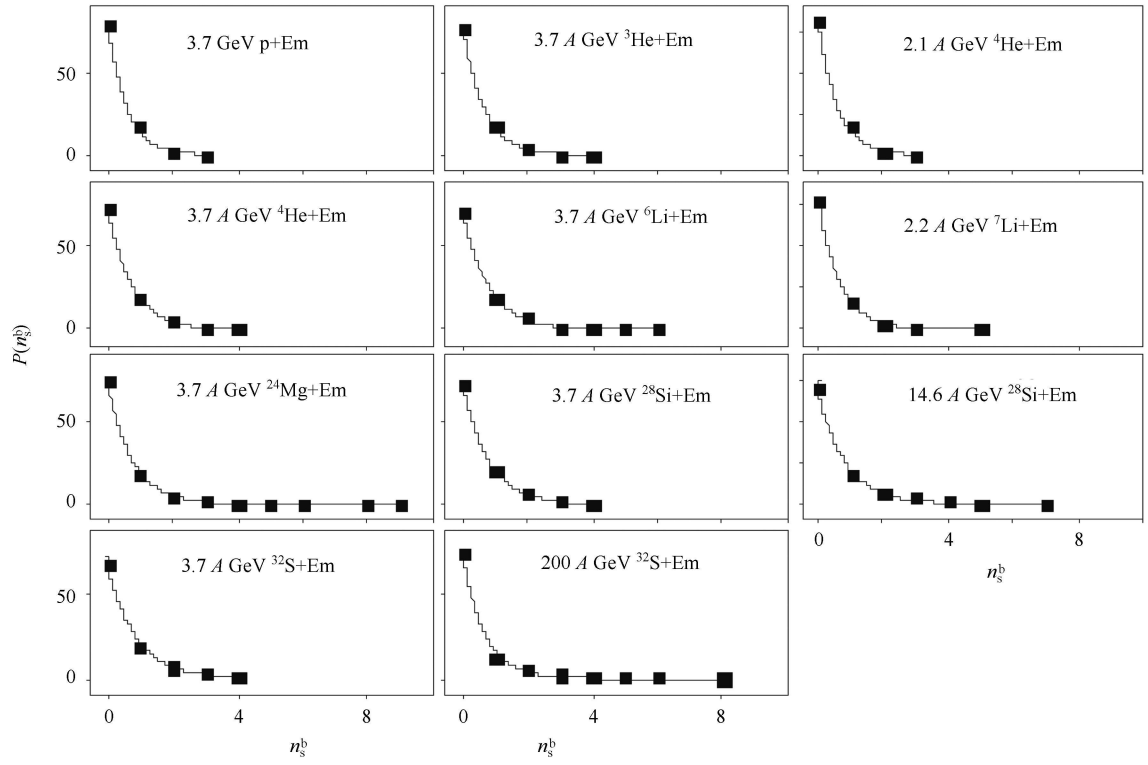

Fig. 2. The multiplicity distributions of the backward emitted shower particle together with the fitted curves.

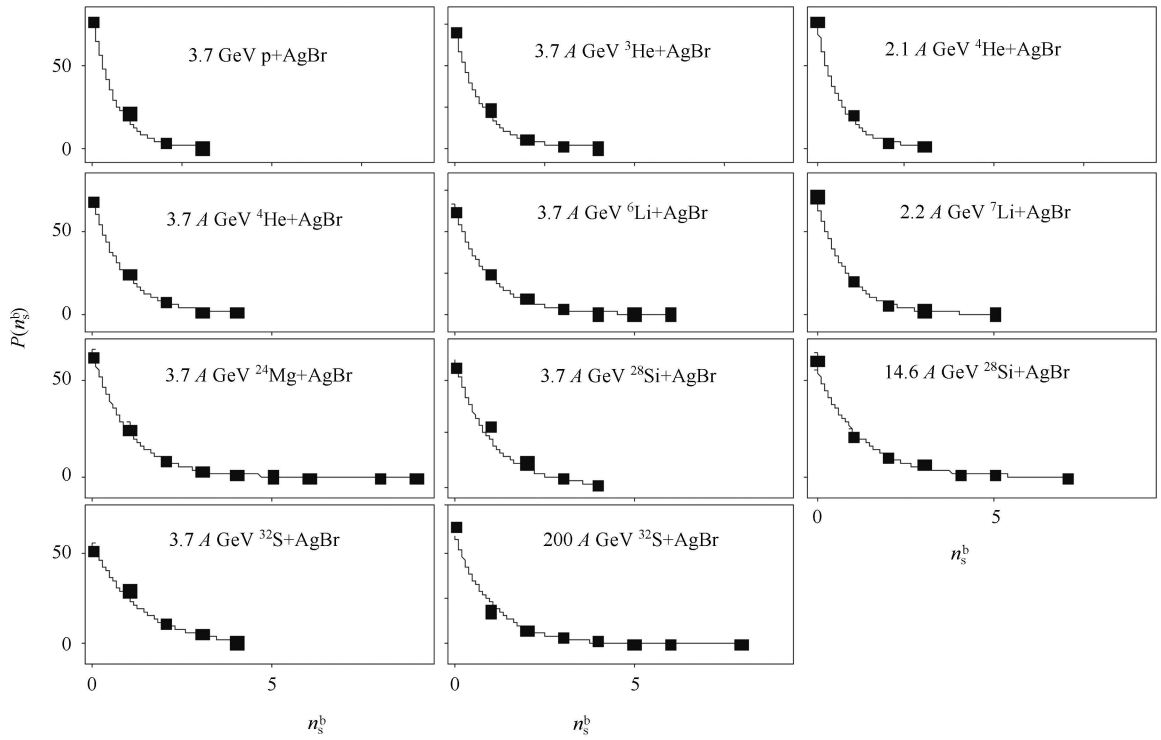

Fig. 3. The multiplicity distributions of the backward emitted shower particle together with the fitted curves.

presented in the figures by the smooth curves.

$$P\left(n_{\rm s}^{\rm b}\right)=p_0{\rm e}^{-\lambda n_{\rm s}^{\rm b}}. \quad (1)$$

The fit parameters p_0 and λ are listed in Table 1. From Table 1 it is found that p_0 is nearly 86.38, 74.36, and 65.87 while λ is nearly 2.02, 1.41, and 1.12 for CNO, Em, and AgBr target nuclei, respectively, irrespective of energy and projectile size. These values are calculated on average. Therefore, the only effective parameter in this production system is the target size and the current behavior can be regarded in the framework of the nuclear limiting fragmentation hypothesis. Accordingly, this particle multiplicity can be correlated with the target size in Fig. 4.

In Fig. 4, the decay constant, λ, and the coefficient parameter, p_0, decrease with the target size. They can be correlated with the target mass number, $A_{\rm T}$, using linear relationships presented by the straight lines. The slope parameters are -0.01 ± 0 and -0.25 ± 0.03, and the intercept values are 2.19 ± 0.09 and 90.31 ± 2.18, respectively, for the dependence of λ on the target size $A_{\rm T}$ and p_0 on $A_{\rm T}$. Therefore, the multiplicity distributions of Eq. (1) can be determined as a function of $A_{\rm T}$. The backward particle emission mechanism of pions and protons was of concern in different experiments [28–30]. Zhan Dong-Hai et al [30] showed that the multiplicity distribution of the backward emitted shower particle is similar in the interactions of 3.7 A GeV ^{12}C, ^{16}O, and ^{28}Si with emulsion nuclei. The independence on the projectile size is regarded in this particle emission system.

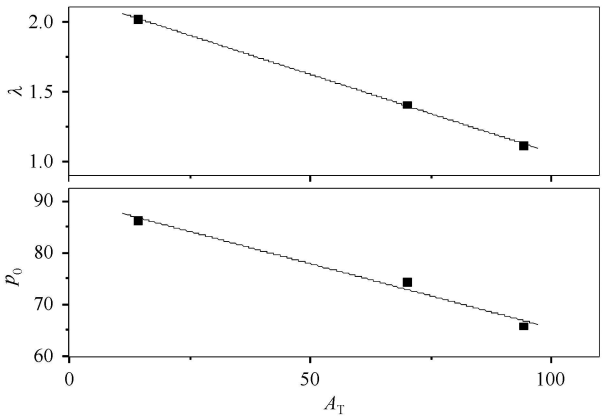

Fig. 4. The characteristic parameters of the backward emitted shower particle distributions as function of the target mass number together with the fitted lines.

3.2 Production probability

The production probability is defined here as the number of events accompanied by an emission of backward shower particles, P ($n_{\rm s}^{\rm b}>0$), normalized to the total number of events. The associated probability for the present interactions is listed in Table 2. From Table 2,

one observes that in the interactions with H, CNO, and Em the probabilities are nearly constant with respect to the projectile size and energy. On average, they are nearly 5.69, 13.77, and 25.16%, respectively, within statistical error. This constancy implies a limited behavior. For the interactions with AgBr, the probability increases with projectile size up to ^{6}Li. At $A_{\rm Proj}\geqslant 6$ the probability tends nearly to a constant limit ∼39.25.

In the basic picture of the high-energy nucleus-nucleus collisions, the target and projectile make an overlapping region. This region contains the participant nucleons from the projectile and target. The nucleons in the overlap region are called participants while those outside of this area are spectators. The size of the participant matter is formed from both the projectile and target nuclei. Hence, the participant matter size can be accounted not only by the size of one of the two colliding nuclei but also by their relative size. Since the participant region is the source of the excitation energy, provided to the target, the relative size of the light projectiles with respect to AgBr allows a smaller-size participant matter. Consequently the target excitation will be insufficient to reach the limitation region.

The dependence of the probability on the target size is displayed in Fig. 5. In Fig. 5 the production probability is correlated with $A_{\rm T}$ by a power law relation of Eq. (2). The correlation is presented by the smooth curves. The fit parameters, a and b, are listed in Table 2. From the results in Table 2, it is found that coefficient a decreases and the power b increases with the increase of the projectile mass or energy.

$$P\left(n_{\rm s}^{\rm b}>0\right)=aA_{\rm T}^{\rm b}. \tag{2}$$

Table 2. The production probability of the backward emitted shower particles in the present interactions.

projectile	$E_{\rm lab}/A$ GeV	H	CNO	Em	AgBr	a	b
p	3.7	4.88±2.44	15.47±1.46	21.10±0.89	24.04±1.14	6.31±1.31	0.29±0.05
^{3}He	3.7	6.41±2.86	12.76±1.56	23.32±1.18	29.67±1.17	4.95±1.38	0.38±0.07
^{4}He	2.1	5.98±2.26	11.96±1.38	19.31±0.97	24.04±1.35	5.27±1.06	0.32±0.05
	3.7	8.07±3.61	16.87±2.23	26.47±1.56	32.67±2.16	7.44±1.32	0.31±0.04
^{6}Li	3.7	6.25±3.13	15.22±2.13	28.56±1.67	38.06±2.48	4.81±1.69	0.44±0.08
^{7}Li	2.2	3.08±2.18	12.84±1.96	21.84±1.48	28.86±2.19	3.64±1.24	0.44±0.08
^{24}Mg	3.7	4.92±2.01	13.83±1.85	25.69±1.53	38.62±2.61	3.38±2.21	0.52±0.15
^{28}Si	3.7	2.19±1.26	14.63±1.89	28.37±1.58	43.87±2.71	2.41±1.98	0.62±0.19
	14.6	10.15±3.83	17.01±2.96	28.80±2.28	41.18±3.77	7.12±3.41	0.36±0.11
^{32}S	3.7	–	10.53±2.25	30.20±2.16	48.60±3.68	0.59±1.01	0.96±0.39
	200	4.95±1.65	10.40±1.47	23.08±1.29	35.55±2.22	2.02±1.77	0.61±0.20

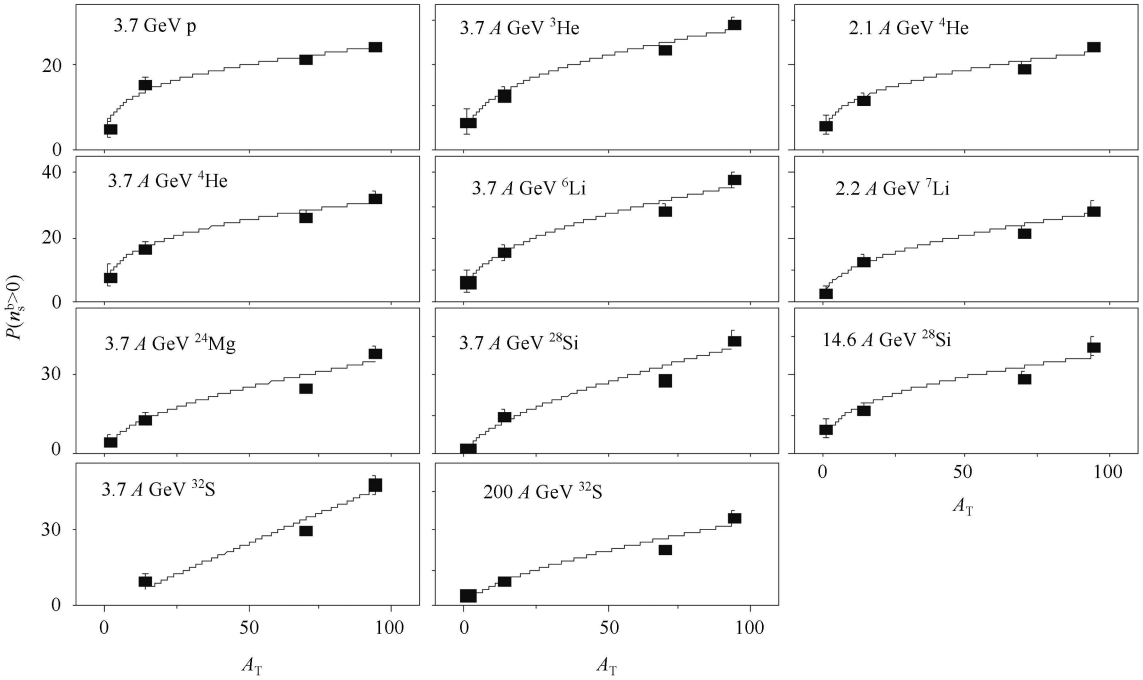

Fig. 5. The backward emitted shower particle production probability as a function of target size in the present interactions, together with the fitting curves.

3.3 Average multiplicity

The average multiplicity values of the backward emitted shower particles through the present interactions are listed in Table 3. In the interactions with H and CNO, the average multiplicity is nearly 0.05 and 0.16, respectively, irrespective of the projectile size and energy. For the interactions with Em and AgBr, the average values increase with the projectile size for the light nuclei up to ^{6}Li. Then, at $A_{\rm Proj}\geqslant 6$ they tend to constancy. They nearly tend to 0.41 and 0.64 for Em and AgBr, respectively. Therefore, the size of the participant matter depends on the relative size between the projectile nucleus and the target nucleus. It plays a main role in the target excitation process and, consequently, in the limitation of the nuclear destruction mechanism. On the other hand, the dependence of the average multiplicity on the target size is presented in Fig. 6. In Fig. 6, the average values are correlated with $A_{\rm T}$ by the power law relation of Eq. (3). The correlation is presented by the smooth curves. The fit parameters, c and d, are listed in Table 3. From Table 3, the values of the coefficient c is decreased and the power d is increased with the increase of the projectile mass. In a similar observation from the data

Table 3. The average multiplicity of the backward emitted shower particles in the present interactions.

projectile	$E_{\rm lab}/A$ GeV	H	CNO	Em	AgBr	c	d
p	3.7	0.05±0.02	0.17±0.02	0.24±0.01	0.27±0.01	0.07±0.01	0.31±0.05
^{3}He	3.7	0.08±0.04	0.14±0.02	0.29±0.01	0.37±0.02	0.05±0.02	0.42±0.09
^{4}He	2.1	0.06±0.02	0.13±0.01	0.22±0.01	0.28±0.02	0.05±0.01	0.36±0.06
	3.7	0.08±0.04	0.18±0.02	0.35±0.02	0.45±0.03	0.06±0.02	0.43±0.07
^{6}Li	3.7	0.06±0.03	0.17±0.02	0.41±0.02	0.57±0.04	0.03±0.01	0.62±0.12
^{7}Li	2.2	0.03±0.02	0.15±0.02	0.29±0.02	0.40±0.03	0.03±0.02	0.53±0.10
^{24}Mg	3.7	0.05±0.02	0.17±0.02	0.40±0.03	0.64±0.05	0.02±0.02	0.75±0.24
^{28}Si	3.7	0.02±0.01	0.16±0.02	0.39±0.02	0.64±0.04	0.01±0.02	0.84±0.28
	14.6	0.05±0.04	0.22±0.04	0.50±0.04	0.76±0.07	0.03±0.03	0.69±0.18
^{32}S	3.7	–	0.12±0.02	0.46±0.03	0.77±0.05	0.01±0.01	1.31±0.47
	200	0.05±0.02	0.12±0.02	0.41±0.02	0.69±0.04	0.01±0.01	1.18±0.40

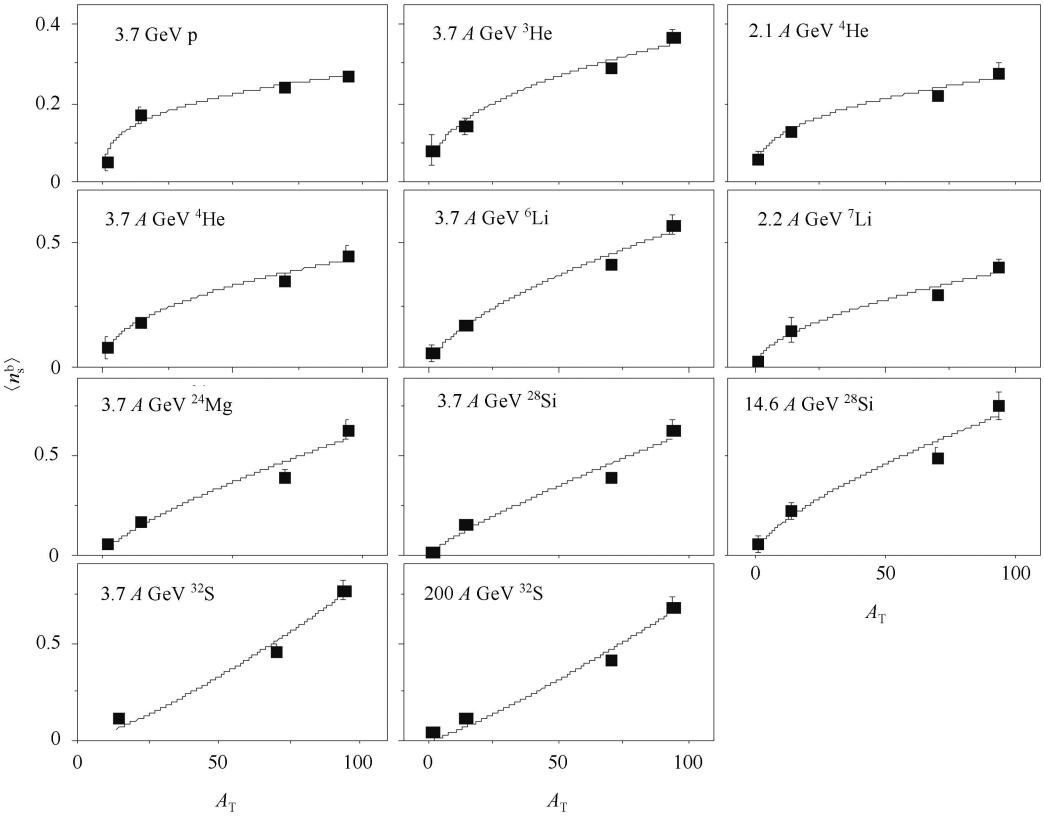

Fig. 6. The dependence of the backward-emitted shower particle average multiplicity on the target size in the present interactions, together with the fitting curves.

of Zhan Dong-Hai et al. [30], it was shown that the average multiplicity of the backward emitted shower particle increases with the projectile mass number up to ^{6}Li in the interactions with emulsion nuclei. At $A_{\rm proj}\geqslant 6$ the saturation was observed where the average multiplicity tends to a constant value ∼0.4.

$$\left\langle n_{\rm s}^{\rm b}\right\rangle = cA_{\rm T}^{d}. \tag{3}$$

4 Conclusion

In a comprehensive way, the universality trend of the backward emitted shower particle production mechanism is confirmed. Accordingly, the used dimensions are the projectile size, the target size, and the incident energy. The data of nuclear collisions with different emulsion nuclei are utilized over a wide range of projectile masses ($A_{\rm Proj}$=1 to 32) and a large energy region ($E_{\rm lab}$=1 A to 200 A GeV). The exponential decay is a characteristic feature of the backward emitted shower particle multiplicity distribution. The decay constant, λ, associated with each target is nearly 2.02, 1.41, and 1.12 for CNO, Em, and AgBr, respectively, irrespective of the projectile size and energy. This decay constant depends linearly on the target size. The backward emitted shower particle production probability is independent on the projectile size and energy. This probability is correlated with the target size in a power law relation. For the interaction with H and CNO, the average multiplicity is 0.05 and 0.16, respectively, irrespective of the projectile size and energy. For the interaction with Em and AgBr, the average multiplicity tends to a saturation at $A_{\rm Proj}\geqslant 6$, where its value is 0.41 and 0.64, respectively. The average multiplicity of the backward emitted shower particle is correlated with the target size in a power law relation. The nuclear limiting fragmentation hypothesis is regarded in this production system, where the target size is the main effective parameter.

This work is carried out at Mohamed El-Nadi High Energy Lab, Faculty of Science, Cairo University, Egypt. The author appreciates the guidance and advice given him by Prof. Dr. A. Abdelsalm, Faculty of Science, Cairo University, Egypt. I wish to acknowledge the kind hands of Vekseler and Baldin High Energy Lab, JINR, Dubna, Russia, for supplying the photographic emulsion plates irradiated at Synchrophasotron. I owe much to the CERN authorities for providing the photographic plates of 200 A GeV ^{32}S, irradiated at SPS.

References

1 Baldin A M, Giordenescu N, Zubarev V N, Ivanova L K, Moroz N S, Povtorelko A A, Radomanov V B, Stavinskiĭ. Sov. J. Nucl. Phys., 1975, **20**: 629
2 Sverker Fredriksson. Phys. Rev. Lett., 1980, **45**: 1371
3 Schroeder L S, Chessin S A, Geaga J V, Grossiord J Y, Harris J W, Hendrie D L, Treuhaft R, van Bibber K. Phys. Rev. Lett., 1979, **43**: 1787
4 Geaga J V, Chessin S A, Grossiord J Y, Harris J W, Hendrie D L, Schroeder L S, Treuhaft R N, van Bibber K. Phys. Rev. Lett., 1980, **45**: 1993
5 El-Nadi M, Ali-Mossa N, Abdelsalam A. IL Nuovo Cimento A, 1998, **110**: 1255
6 El-Nadi M, Abdelsalam A, Ali-Mossa N, Abou-Moussa Z, Kamel S, Abdel-Waged Kh, Osman W, Badawy B. Eur. Phys. J. A, 1998, **3**: 183
7 El-Nadi M, Abdelsalam A, Ali-Mossa N, Abou-Moussa Z, Abdel-Waged Kh, Osman W, Badawy B. IL Nuovo Cimento A, 1998, **111**: 1243
8 Abdelsalam A, Shaat E A, Ali-Mossa N, Abou-Mousa Z, Osman O M, Rashed N, Osman W, Badawy B M, El-Falaky E. J. Phys. G: Nucl. Part. Phys., 2002, **28**: 1375
9 Abdelsalam A, Badawy B M, El-Falaky E. Can. J. Phys., 2007, **85**: 837
10 Abdelsalam A, El-Nagdy M S, Badawy B M. Can. J. Phys., 2011, **89**: 261
11 Abdelsalam A, Badawy B M, Hafiz M E. Can. J. Phys., 2012, **90**: 515
12 Abdelsalam A, Badawy B M, Hafiz M E. J. Phys. G: Nucl. Part. Phys., 2012, **39**: 105104
13 Benecke J, CHOU T T, YANG C N, YEN E. Phys. Rev., 1969, **188**: 2159
14 Powell C F, Fowler F H, Perkins D H. The Study of Elementary Particles by The Photographic Method. Pergamon Press. London, New York, Paris, Los Angles, 1958. 474
15 Barkas H. Nuclear Research Emulsion, Vol. I, Technique and Theory Academic Press Inc., 1963
16 Dipak Ghosh, Argha Deb, Srimonti Dutta. Phys. Scr., 2009, **79**: 025102
17 Dipak Ghosh, Argha Deb, Srimonti Dutta. FIZIKA B, 2007, **16**: 67
18 Dipak Ghosh, Argha Deb, Srimonti Dutta. Can. J. Phys., 2009, **87**: 311
19 Dipak Ghosh, Argha Deb, Ruma Saha, Rupa Das. Can. J. Phys., 2010, **88**: 651
20 El-Naghy A et al. J. Phys. G: Nucl. Part. Phys., 1988, **14**: 1125
21 El-Nagdy M S, Abdelsalam A, Abou-Moussa Z, Badawy B M. Can. J. Phys., 2013, **91**: 737
22 Barashenkov V S, Toneev V D. Interactions of High Energy Particles and Atomic Nuclei with Nuclei, Moskva, Adomizdat, 1972, **12**: In Russian.
23 Florian J R et al. Report Submitted to the Meeting of Division of Particles and Fields, Berkeley, California. 1973
24 Abdelsalam A. JINR Report (Dubna), 1981, E1-81-623
25 Abdrahmanov E O et al. Z. Phys. C, 1980, **5**: 1
26 EMU01 Collaboration; Lund University Report, Sweden, LUIP 8904, May 1989
27 Shmakov S Yu, Uzhinskii V V. Com. Phys. Comm., 1989, **54**: 125
28 GAO Yan, LIU Fu-Hu, Abd Allah N N, Bekmirzaev R. Chinese Physics C, 2011, **35**: 40
29 LI Jun-Sheng, ZHANG Dong-Hui, LIU Fu-Hu. Chinese Physics C, 2008, **32**: 352
30 ZHANG Dong-Hai, ZHAO Hui-Hua, LIU Fang, HE Chun-Le, JIA Hui-Ming, LI Xue-Qin, LI Zhen-Ya, LI Jun-Sheng. Chinese Physics, 2006, **15**: 1987